Original Article

Determination method of permafrost table in seasonal frozen soil areas under "Water-Heat-Salt" coupling

WANG Fang[1] https://orcid.org/0000-0003-1856-9855; e-mail: fangwang@ahjzu.edu.cn

YANG Zhong[1] https://orcid.org/0009-0004-9686-6702; e-mail: 497447480@qq.com

LIU Kai[2]* https://orcid.org/0000-0003-3916-0303; e-mail: liukai@hfut.edu.cn

LU Chang-long[1] https://orcid.org/0009-0006-5927-1261; e-mail: 2758124752@qq.com

*Corresponding author

1 School of Civil Engineering, Anhui Jianzhu University, Hefei 230601, China

2 School of Automobile and Traffic Engineering, Hefei University of Technology, Hefei 230009, China

Abstract: The permafrost table is an important index for the design and construction of roads in cold regions, so it is necessary to find a convenient, accurate and fast judgment method to determine the permafrost table. In this study, a three-field coupled model was established based on the hydrothermal salt coupling within the permafrost and the similarity theory, and the changes of the permafrost table under different temperature, moisture and salt conditions were numerically simulated by considering the transient temperature change and the influence of the permafrost layer on the seasonally thawed layer. In addition, an accelerated permafrost table test method was designed based on the time-domain variation and hydrothermal salt coupling by the similarity theory, which rapidly simulated the permafrost table change under different temperatures, moisture, and salts in the natural environment. Comparing the simulation and test results with the measured values in the field, the errors are less than 3%, which verified the feasibility of the method for determining the permafrost table, and the simulated results are better than the test results. Results show that the results of

determining the permafrost table with a single index have different degrees of deviation, and the permafrost table obtained by the temperature index is the most accurate in general, and it is more accurate to use the average value of the three indexes as the permafrost table compared with a single index.

Keywords: Permafrost table; Hydrothermal salt coupling; Seasonally thawed layer; Numerical simulation; Accelerated test

1 Introduction

Frozen soil refers to rock and soil containing ice below zero centigrade (Obu 2021). The layers from top to bottom are the seasonally thawed layer and permafrost layer (Shiklomanov et al. 2013; Dobinski 2020), as shown in Fig. 1. The seasonally thawed layer is close to the ground surface, which is characterized by winter freezing and summer melting. The permafrost layer is far away from the ground surface and remains permanently frozen (Ryan et al. 2018). The maximum depth from the ground surface to the top of the permafrost layer in a year is the permafrost

table, which is the maximum thaw thickness of seasonally thawed layer. With global warming, the permafrost degrades year by year, and the thickness of the seasonally thawed layer increases (Zhao et al. 2019; Peng et al. 2015). The seasonally thawed layer expands and melts with the temperature, leading to thaw settlement, frost heave, potholes and cracks (Liu et al 2019). Changes in the permafrost table directly reflect the activity of the seasonally thawed layer. Therefore, the determination of the permafrost table is important for the prevention and control of road diseases in cold regions.
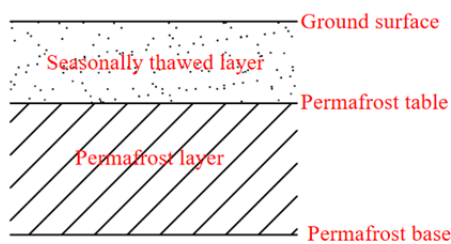

Fig. 1 Vertical distribution of permafrost in summer.

At present, the main methods to determine the permafrost table are the drilling method, radar detection method and empirical formula method (Qi et al. 2023; Yang et al. 2018; Xu et al. 2005). Although the drilling method has high measurement accuracy, the construction period is long and difficult and will damage the local ecosystem (Romanovsky et al. 2010). The radar detection method is convenient to measure, but its accuracy still needs to be determined by field test (Daout et al. 2017; Jia et al. 2017). The empirical formula method is summarized and fitted by a large number of measured data, but the obtained error of the permafrost table is large and lacks credibility (Romanovsky et al. 2010). Therefore, it is essential to propose a convenient, accurate and fast method for determining the permafrost table.

In order to obtain better permafrost table determination than traditional method, it is necessary to study the variation of the permafrost table change under multifactorial conditions. The factors influencing the change of the permafrost table include external and internal factors. External factors include the impact of human activities and environmental changes (Rasmussen et al. 2018; Kong et al. 2018; Zhang et al. 2020). The internal factors include the effects of solid, liquid and heat during the freezing and thawing of frozen soil and their coupling effects. To determine the change law of the permafrost table, it is necessary first

to understand the changes of external environment and the internal change mechanism of soil in the process of freezing and thawing. Multiple studies have found that the conductivity of water during freezing and expansion had a significant effect on solute migration and ice separation, and that solute transfer depended to a large extent on the movement of unfrozen water, by utilizing the electrical conductivity method and pH value can monitor the movement pattern of ions during the freezing and thawing , thus obtaining the salt transport pattern during the freezing and thawing (Ming et al. 2016; Bing et al. 2019; Shafique et al. 2016). In order to further study the influence of multiple factors on the permafrost table, some scholars have established salinity field model, considered the influence of climate change on hydrothermal salt transport, numerically simulated the coupled transfer of water, heat, and solute in freeze-thawed saline soils, and predicted the influence of future temperature and precipitation changes on hydrothermal salt transport in unsaturated permafrost (Xu et al. 2020; Wan et al. 2021). Most studies have focused on the effects of coupled hydrothermal salt action on permafrost frost heave and thaw settlement at steady-state ambient temperatures, while neglecting the effects of coupled hydrothermal salt action on the permafrost table at dynamically cycling ambient temperatures. In addition, the research on the permafrost table focused on the seasonally thawed layer. Zhu et al. (2022) modeled the permafrost table changes induced by train vibrations under different global warming conditions, and the freezing and thawing temperature was constant. Zhang et al. (2022) studied the change in the permafrost table under the influence of snowpack, ignoring the impact of the permafrost layer on the seasonally thawed layer, this was different from the change in the permafrost table under natural conditions.

In this study, we established a three-field coupled model based on the hydrothermal salt coupling within the permafrost and the similarity theory, and considered the transient temperature change and the influence of the permafrost layer on the seasonally thawed layer, and numerically simulated the change of the permafrost table under different temperature, moisture and salt. In addition, an accelerated permafrost testing method based on time-domain variation and hydrothermal salt coupling was designed using similarity theory to rapidly simulate the permafrost table changes under different temperatures, moisture and salts in the natural environment.

Comparing the simulation and test results with the field measured values of the permafrost table in the Hulun Beier Mountains to the west of the Daxing'anling Mountains, the feasibility of the method to determine the permafrost surface was verified, and a convenient, accurate and rapid method to determine the permafrost water level was obtained by analyzing the error of the permafrost table determined by a single index and multiple indexes.

2 Determination Method of Permafrost Table

To determine the position of the maximum melting depth of the soil in a year, and that is the position of permafrost table.

The following assumptions were made for the theoretical model according to the actual situation.

(1) Water movement in soil conformed to Darcy's law.

(2) Assuming that the soil was homogeneous and had the same properties in all directions, only the temperature, moisture and salt content changes in the vertical direction were considered.

(3) There was only vertical temperature conduction, the conduction medium was soil skeleton, water and ice.

(4) The effects of water evaporation, salt precipitation, frost heave and solid ice on liquid water and salt in water were not considered.

(5) Moisture migration in frozen soil moved in liquid form, and the ice was considered fixed.

(6) Closed without external hydration.

The flow chart of determination method is shown in Fig. 2.

2.1 Governing equation for heat transfer and parameters

According to the energy conservation law and the Fourier heat transfer law, the latent heat of phase change was used as a heat source to deal with the heat transfer during the freezing or thawing process of unsaturated soils. Thus, the differential equations of frozen soil heat conduction (Harlan 1973) can be expressed as Eqs. (1) and (2)

$$C \frac{\partial T}{\partial t} = \frac{\partial}{\partial z}\left(\lambda(\theta) \frac{\partial T}{\partial z}\right) + L\rho_i \frac{\partial \theta_i}{\partial t} \qquad (1)$$

$$\theta = \frac{\rho_i}{\rho_w}\theta_i + \theta_u \qquad (2)$$

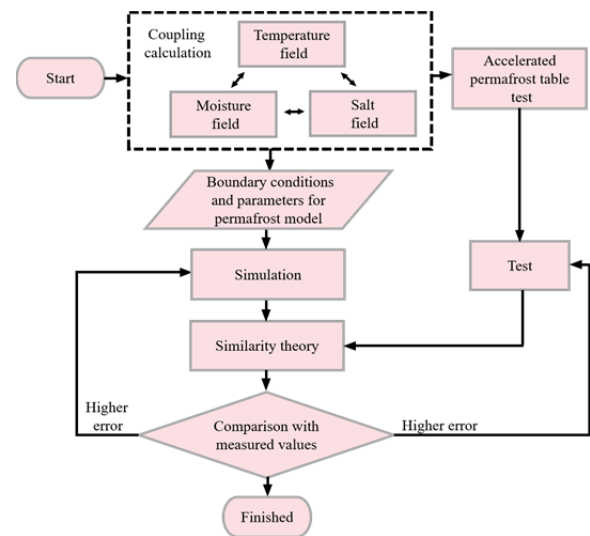where T is the instantaneous temperature of soil mass

Fig. 2 Flow chart of determination method.

(°C); t is time (s); θ_i is pore ice volume content; θ_u is the volume content of unfrozen water; z is depth direction coordinates (m); ρ_i is the ice density; ρ_w is the water density; L is the latent heat during phase change from water to ice (kJ/kg); λ is the heat conductivity(J/(hm °C)); C is the volumetric heat capacity (J/(kg °C)).

The specific heat of the soil can be expressed by volume-weighted averages of various material components, while the heat conductivity has an exponentially weighted nature. Assuming that the soil skeleton index is the same in the freeze-thaw state, the volumetric specific heat C and heat conductivity λ can be described as Eqs. (3) and (4)

$$C = C_s\rho_s\theta_s + C_i\rho_i\theta_i + C_w\rho_w\theta_u \qquad (3)$$

$$\lambda = \lambda_s^{\theta_s}\lambda_w^{\theta_u}\lambda_i^{\theta_i} \qquad (4)$$

where C_s, C_w, C_i are the mass heat capacity of soil particles, unfrozen water and ice (J/(kg °C)); ρ_s is the soil particle density; θ_s is the soil particle volume content; λ_s, λ_s, λ_s are the heat transfer coefficients of soil particles, unfrozen water and ice (J/(hm °C)). According to reference (Xu et al. 2020), C_S =2217, C_w =4180, C_i =1874, λ_S =1.18, λ_w =0.58, λ_i =2.22.

The temperature at the location of the permafrost table is 0°C, so the depth from the location of 0°C to the surface is taken as the value of the permafrost table.

2.2 Governing equation for unfrozen water migration and parameters

According to the thermodynamic principles, soil water potential is the fundamental cause of soil water

movement, which is generally composed of gravity potential, pressure potential, matrix potential, solute potential and temperature potential. For unsaturated frozen soil, only the effects of matrix potential and gravity potential were considered (Harlan 1973), and the motion equation of unfrozen water can be expressed as Eqs. (5) and (6)

$$\frac{\partial \theta_u}{\partial t} + \frac{\rho_i}{\rho_w}\frac{\partial \theta_i}{\partial t} = \frac{\partial}{\partial z}(k\frac{\partial \psi}{\partial z}) \qquad (5)$$

$$\psi = \psi_w + z_0 \qquad (6)$$

where k is the permeability coefficient of soil (m/h); ψ is soil water potential (m); ψ_w is soil matric potential (m); z_0 is soil gravitational potential (m).

Based on the soil water potential theory of unsaturated soil (Vereecken et al. 2010), k and ψ_w can be expressed as Eqs. (7) and (8)

$$k(s) = k_0 S^a[1-(1-S^{\frac{1}{m}})^m]^2 \times l \qquad (7)$$

$$\psi_w = c\theta_u^{-d} \qquad (8)$$

where k_0 is soil permeability under saturated state (m/h); a, m, c, d depend on the nature of the soil (Lu and Likos 2004), k_0 =2.5×10^{-6} , a=0.5, m=0.25, c=0.106, d=6.0532; S is the relative saturation of unsaturated soil.

The relative saturation of unsaturated soil can be expressed as Eq. (9)

$$S = \frac{\theta_u - \theta_r}{\theta_s - \theta_r} \qquad (9)$$

where θ_s is the saturated water content; θ_r is the residual water content.

The impedance factor I indicates that the migration and transport of unfrozen water in the soil will be hindered by solid pore ice (Genuchten 1980), which can be expressed as Eq. (10).

$$I = 10^{-10\theta_i} \qquad (10)$$

The theoretical model is in a closed environment with no rehydration, with the increase of temperature, the soil begins to melt, the unfrozen water content increases gradually, and moves downward under gravity. The permafrost layer below has a good water insulation effect, and the unfrozen water in the soil cannot continue to move downward, at this time, unfrozen water is at its maximum. This location is at the top of the permafrost layer, which is considered to be the permafrost table.

2.3 Governing equation for salt migration and parameters

Solute migration mainly comes from two aspects:

one is convective migration accompanied by water movement due to concentration gradients, and the other is solute diffusion. It can be represented as Eq. (11)

$$\frac{\partial(c\theta_u)}{\partial t} = \frac{\partial}{\partial z}(D_{sh}\frac{\partial c}{\partial z}) \qquad (11)$$

where c is the solute concentration (g/L); D_{sh} is hydrodynamic dispersion coefficient, including the molecular diffusion coefficient of solute hydrodynamic diffusion D_i and mechanical diffusion coefficient $D_{m.}$

For unsaturated soil, when the water content is low, the molecular diffusion coefficient decreases, because the volume of liquid in the soil decreases. Therefore, D_i can be given as a function of water content (Dong et al. 2018; Ren et al. 2017), as shown in Eq. (12)

$$D_i = D_0 a_1 e^{b_1\theta} \qquad (12)$$

where D_0 is the diffusion coefficient of solute in free water (m^2/h); a_1, b_1 are empirical parameter related to soil property, based on the literature (Ren et al. 2017), D_0=1.098×10^5, a_1=0.00261, b_1=10.

The mechanical diffusion coefficient D_m is simplified to be linearly correlated with seepage velocity, which can be expressed as Eq. (13)

$$D_m = \beta|v| \qquad (13)$$

where β is the degree of dispersion (m), based on the literature (Ren et al. 2017), β=7.021× 10^{-3} ; v is the mean seepage velocity in soil pores (m/h).

The location of the permafrost table has the highest salt content, so the depth from the location with the highest salt content to the surface is used as the value for the permafrost table.

2.4 Determination of permafrost table under coupling of hydrothermal salt

According to Eq. (1), Eq. (5) and Eq. (11), the unknowns in the equations were θ_i, θ_u, T, c. Therefore, to establish the relationship between the four unknowns, the unfrozen water content in the permafrost was estimated, as shown in Eq. (14)

$$\frac{w_0}{w_u} = (\frac{T}{T_f})^B \qquad (14)$$

where w_0 is the initial water content of frozen soil (%); w_u is unfrozen water content (%); T_f is the freezing temperature of soil (°C); B is an empirical parameter dependent on soil property, B = 0.56 for clayey soils (Lu and Likos 2004).

Referring to the solid-liquid ratio, the volume

ratio of pore ice to unfrozen water in frozen soil was defined as solid-liquid ratio B_i , which can be expressed as Eq. (15)

$$B_i = \frac{\theta_i}{\theta_u} = \begin{cases} 1.1(\frac{T}{T_f})^B - 1.1 & T \le T_f \\ 0 & T > T_f \end{cases} \quad (15)$$

Eq. (15) shows that the solid-liquid ratio B_i is a piecewise function of temperature T, so the relationship between θ_i, θ_u, T can be expressed as Eq. (16).

$$\theta_i = B_i(T) \times \theta_u \quad (16)$$

Combined with Eq. (1), Eq. (5), Eq. (11) and Eq. (16), the finite element method was used for numerical solution to obtain the temperature, moisture and salt content data at different times and heights under the hydrothermal salt coupling conditions.

3 Permafrost Table Theoretical Modeling

3.1 Similarity theory

The change of the permafrost table is a long-term process, taking a decade or even decades. To speed up the research process, the actual conditions of permafrost can be translated into test conditions based on similarity theory. The specimen size and test time can be determined according to the thickness of the seasonally thawed layer of permafrost under natural conditions, laboratory instrument accuracy and mold height.

According to heat conduction theory (Jin et al. 2004), the mathematical model of frozen soil thermal state and single value condition can be described Eq. (17)

$$\lambda^- \left(\frac{\partial T^-}{\partial y} - \frac{\partial T^-}{\partial x} \frac{\partial h}{\partial x} \right) - \lambda^+ \left(\frac{\partial T^+}{\partial y} - \frac{\partial T^+}{\partial x} \frac{\partial h}{\partial x} \right) = Q \frac{\partial h}{\partial x} \quad (17)$$

where x, y, t are independent variables; T^+, T^- are temperature of thawing soil and frozen soil; λ^+, λ^- are thermal conductivity of melted soil and frozen soil; h is melting depth.

Using the similarity transform method (Zhou et al. 1999) to deal with Eq. (17), three similarity criteria can be obtained: the Fourier number $F_0 = \frac{at}{l}$, the Nusselt Number $N_u = \frac{an}{\lambda_g}$, and the temperature criteria $\theta_0 = \frac{T_a}{T}$. Where T_a is ambient temperature, λ_g is thermal conductivity, a is coefficient of heat convection. Relationships among the similarity

constants are

$$\frac{c_l^2}{c_a^2 c_t^2} = 1 \; , \qquad \frac{c_Q c_l^2}{c_\lambda c_T c_t} = 1 \quad (18)$$

where, C_a is similarity constant of thermal diffusivity; C_t is time similarity constant; C_l is eometric similarity constants; C_Q is similarity constant of the coefficient of heat convection; C_λ is similarity constant of the thermal conductivity; C_T is temperature similarity constants.

The same soil with the same initial moisture content as the original soil is used as the medium, at this time, $C_a = C_\lambda = C_Q = 1$. when $C_T = 1$, the temperature change of soil was as the same as the original soil, so $C_a = C_l^2$. When the soil property of the model was the same as the original soil, the time scale of model test was the square times of model height scale, and the freeze-thaw depth scale of the model was the same as the height scale of the model. The height of the test mold was 23 cm, and the height of the seasonally thawed layer under natural conditions measured on site was 1.8-2.6 m, so the geometric ratio was preliminarily determined to be 1:20. At this time, C_l is reduced by a factor of 20. Based on the relationship between the similarity constants, the time C_t needed to be scaled down by a factor of 400, so the variation of the permafrost table for one month under natural conditions takes only 2 hours under numerical simulation and indoor test conditions. The permafrost table obtained from simulations and tests can be converted into the corresponding permafrost table under natural conditions, with a conversion factor of 20.

3.2 modeling

The coefficient partial differential equation module PDE in COMSOL software was used for secondary modeling calculation, Eq. (1), Eq. (5) and Eq. (11) were converted into coefficient type partial differential equations, as shown in Eq. (19).

$$\begin{cases} C(\theta) \frac{\partial T}{\partial t} + \nabla \cdot (-\lambda \nabla T) - L\rho_i \frac{\partial \theta_i}{\partial t} = 0 \\ \frac{\partial \theta_u}{\partial t} + \nabla \cdot (-k \nabla \psi) + \frac{\rho_i}{\rho_w} \frac{\partial \theta_i}{\partial t} = 0 \\ \frac{\partial (c\theta_u)}{\partial t} + \nabla \cdot (-D_{sh} \nabla c) + \nabla \cdot c(-k \nabla \psi) = 0 \end{cases} \quad (19)$$

The numerical simulation scheme was based on the temperature change from 2007.10 to 2021.12 in the Hulun Beier to the west of the Daxing'anling Mountains. The specific location of the monitoring site is on Kudur Mountain at longitude 122°42'36''E,

latitude 50°1'47"N, and elevation of 982 m. The field temperature was divided into 2007.10-2011.12, 2012.10-2016.12 and 2017.10-2021.12 as the simulated boundary temperature. Because the temperature change trend in this area conformed to the sine function, the temperature change in each cycle was fitted to better describe the temperature change trend with time. After measurement, the initial permafrost table in 2007 was 1.92 m, and the initial permafrost table in 2012 was 2.1 m, and the initial permafrost table in 2017 was 2.2 m. The moisture and salt content of soil samples in permafrost and seasonally thawed layer were consistent with the field measured data, and we use sodium chloride as the base salt. According to the field data, unfrozen water contents were 25%, 30% and 35%, respectively. The salt contents were 0.5%, 1% and 1.5%, respectively. The specific numerical simulation schemes of the seasonally thawed layer were shown in Table 1. The water content of the permafrost layer was 10%, salt content was 0.8%.

The size of the test mold is shown in Fig. 3. The height and diameter of the mold were determined based on specification MT-T 593.1-2011, measured data in the field and previous studies (Jia BX et al. 2020; Ji Y et al. 2017). The spacing and size of the curved holes and round holes were based on the size of the sensors we used and earlier research. The height of the seasonally thawed layer and permafrost layer were calculated according to the initial permafrost table in different temperature ranges and the determined geometric ratio. The height of the seasonally thawed layer was 9.6 m, 10.5 m and 11 m, corresponding to three temperature cycles. The upper boundary condition of the model was the temperature change function of the seasonally thawed layer in different temperature cycles. Based on local measured data, the measured ranges of water content, temperature and salt content of permafrost layer were 8.6% to 12.1%, -3.6°C to 2.7°C, and 0.72% to 0.85%, respectively, We chose the middle of three ranges as the initial water content, temperature and salt content of the simulated permafrost layer, which were 10%, -3°C and 0.8%, respectively. The surrounding boundary conditions are enclosed, free of moisture and salt supplementation. According to the field earth

Table 1 Orthogonal scheme of seasonally thawed layer research under different conditions

Time	2007-2011			2012-2016			2017-2021		
Temperature	$T(t) = -0.25 + 18.7\sin(\frac{2\pi}{12} + \frac{2\pi}{3})$			$T(t) = -0.25 + 18.4\sin(\frac{2\pi}{12} + \frac{2\pi}{3})$			$T(t) = -0.36 + 18.8\sin(\frac{2\pi}{12} + \frac{2\pi}{3})$		
water	25%	30%	35%	25%	30%	35%	25%	30%	35%
salt	0.5%	1%	1.5%	1%	1.5%	0.5%	1.5%	0.5%	1%
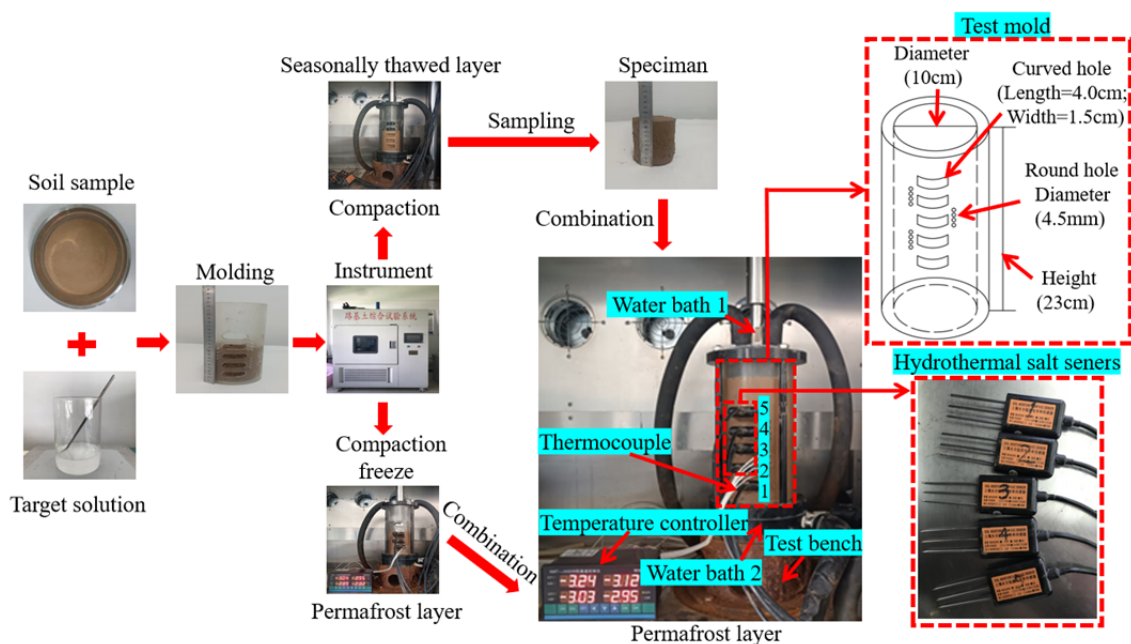
Fig. 3 Procedure diagram of permafrost test.

(a) Geometric model　　　　　(b) Mesh division
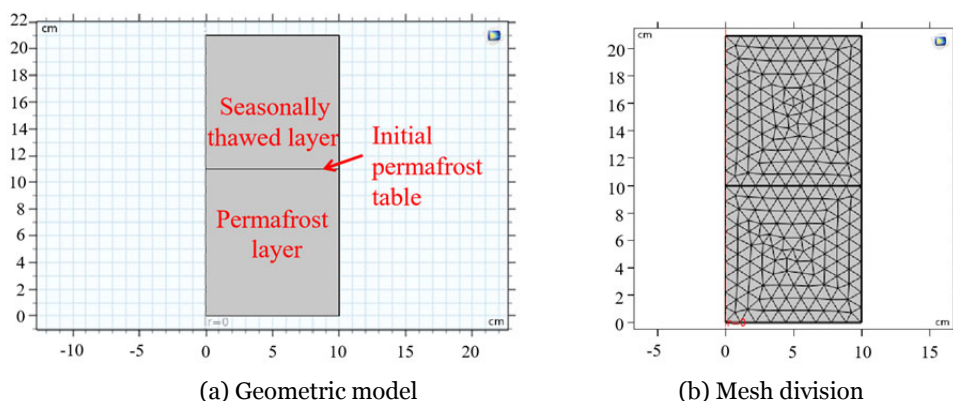
Fig. 4 Modeling and meshing in numerical simulation.

(a) Moisture　　　　　(b) Temperature　　　　　(c) Salt content
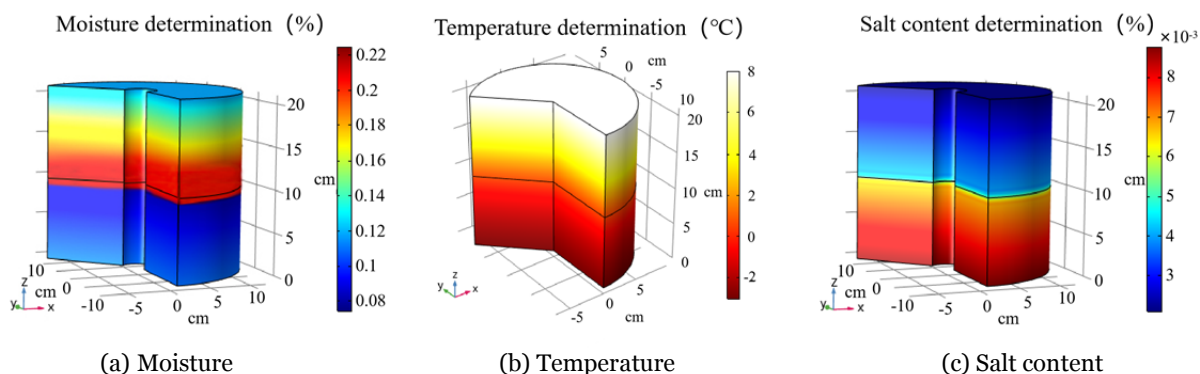
Fig. 5 Distribution cloud maps for different indexes.

pressure, the cross-section pressure of the model was calculated to be 0.5 kN. The established geometric model and mesh division were shown in Fig. 4. Based on Literature (Xu et al. 2001), phase change latent heat was 334500 (J/kg), the density of permafrost in thawing layer was 1600 (kg/m³), the density of permafrost was 1900 (kg/m³), the density of water was 1000 (kg/m³), the density of ice was 900 (kg/m³). The permafrost tables can be determined by the different indexes respectively from the corresponding distribution cloud maps, as shown in Fig. 5.

4　Permafrost Table Test

To further verify the correctness of the method for determining the permafrost table, a permafrost table test was carried out. The test schemes were shown in Table 1. Preparing three identical test pieces under the same test conditions, and the average value of the permafrost table of the three tests were calculated.

Specimen Preparation was divided into two parts: the upper layer of the seasonally thawed layer and the lower layer of permafrost layer, as shown in Fig. 4. The

production process was as follows (Fig. 3).

1. Raw material preparation. Soil samples were taken from the Hulun Beier Mountains, which were dried and ground in a grinder. Removing impurities through a sieve with a diameter of 2mm, and putting soil samples into sealed bags for use.

2. Production of seasonally thawed layer. A quantitative soil sample was weighed into a basin. The mass of distilled water and NaCl crystals required for weighing were calculated according to the Table 1 test protocol, they were mixed and the solution was stirred thoroughly with a glass rod until the NaCl crystals were completely dissolved. The configured solution was evenly sprayed on the soil surface using a spray bottle, and the soil was continuously stirred during the spraying process to ensure uniform distribution of soil moisture and salts. Putting the configured soil sample into the test mold, and compacting the soil sample to the necessary test height, putting the mold into the operating platform for testing. Water bath 2 was below the sample and set at 0°C, water bath 1 was above the sample. Adjust the height of the displacement sensor to make it closely combined with water bath 1, and applying constant force to compress

the soil sample of the seasonally thawed layer. When the displacement sensor reading remained stable, the preparation of the seasonally thawed layer was completed. After completion, taking out the seasonally thawed layer and putting it into the incubator for heat preservation.

3. Production of permafrost layer. The production steps of the permafrost layer were the same as the seasonally thawed layer. The water content was 10%, salt content was 0.8%. When the permafrost layer was compacted, we inserted No. 1, No. 2 and No. 3 hydrothermal salt sensors into the test piece from bottom to top. Set the temperature of water bath 1 and water bath 2 to -20°C to freeze the soil sample of the permafrost layer. When the temperature in the soil was -3°C, the temperature of water bath 1 was turned off, setting the temperature of water bath 2°C to -3°C. The fabrication of the test piece of the permafrost layer was completed.

4. Combination. Adjust the height of the displacement sensor, and taking out the seasonally thawed layer in the incubator, then place it above the permafrost layer. Insert the No.4 and No.5 hydrothermal salt sensors into the soil samples of the seasonally thawed layer from bottom to top, respectively. Insert four thermocouples at appropriate locations according to the test scheme to measure the temperature at different soil locations. Set the temperature of water bath 1 to the desired temperature according to the test scheme. During the test, soil moisture and salt content were collected in real time by hydrothermal salt sensors No. 1 to No. 5 inserted into the soil, the hydrothermal salt sensors were shown in Fig. 3. Combined with the similarity theory, the hydrothermal salt sensor data were collected every 0.6 hours, which was equivalent to every 10 days under natural conditions, and the data can be collected 36 times per year, and the maximum value of the permafrost table obtained from these 36 data was used as the permafrost table for the year.

Based on the sensor temperature and thermocouple data, Soil temperature can be obtained anytime. The conduction law of temperature in soil can be obtained through calculation. When the permafrost reached the maximum thawing depth, the permafrost temperature was 0°C. The permafrost table could be determined by drawing temperature curves at different depths to determine the position of 0°C in the soil, as shown in Fig. 6. According to the data of soil water content at different heights in the
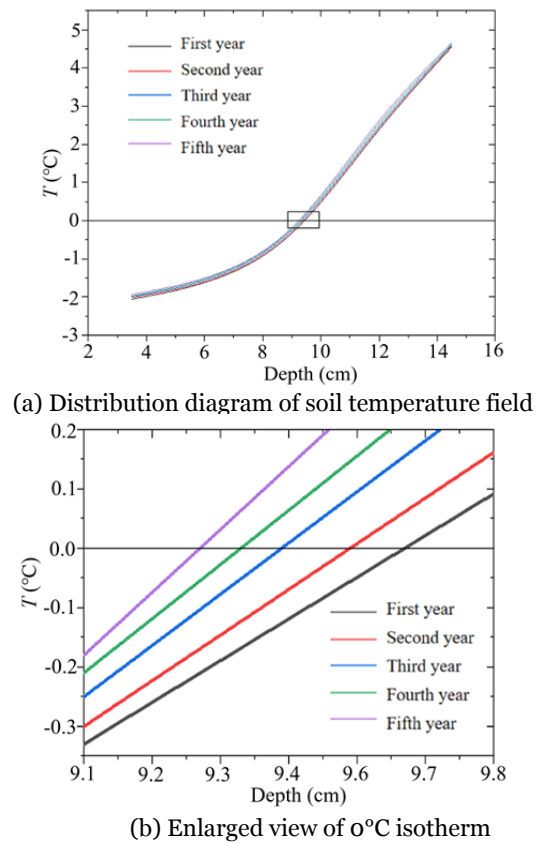

(a) Distribution diagram of soil temperature field

(b) Enlarged view of 0°C isotherm

Fig. 6 Test temperature distribution diagram from 2017 to 2021.

process of soil freezing and thawing cycles, the location of the permafrost table can be tentatively inferred to be between the two sensors.

5. At the end of the freeze-thaw cycle, the soil sample was taken out and the surplus soil sample was cut off. The soil samples at the preliminarily determined permafrost table height were uniformly sliced from top to bottom with a thickness of 2 mm, and put into aluminum boxes for weighing. The quality was M_i. The weighted soil was dried in an oven for 4 hours and then weighed again, the quality was m_i. The height of the maximum water content in the soil can be obtained by comparing the quality difference of the soil samples weighed twice at different heights. The steps were shown in Fig. 7.

6. After the sliced soil samples are dried in an oven, the soil samples of the same quality were weighed from different aluminum boxes and placed in a beaker. A sufficient amount of distilled water was added according to the ratio of 1:5. The samples were fully stirred with a glass rod. After the stirring was completed, the samples were immediately filtered. The filtrate of the same quality was taken with a

dropper and placed in a dry beaker for the water bath, drying and weighing. The location of the maximum salt content in the soil sample was determined by comparing the residual salt mass of different aluminum box soil samples after the above operation, to determine the position of the permafrost table.

5 Results and Discussions

5.1 Permafrost table determined by temperature

In Fig. 8, the results showed that with the increase of freezing and thawing time, the permafrost table increased gradually, and the increase rate decreased

gradually. As the temperature rises, the seasonally thawed layer begins to melt, the unfrozen water moves downward gradually under gravity, and a large amount of heat is carried. Meanwhile, as the thickness of the seasonally thawed layer increases, and the unfrozen water content above decreases gradually. Since the thermal conductivity of water is higher than that of the soil, the thermal conductivity of the seasonally thawed layer decreases, thus the heat conduction of the bottom weakens, and the permafrost table gradually stabilizes, the changing pattern is the same as the permafrost table under natural condition. The values of the permafrost table obtained by simulation and test are lower than the natural conditions. The reason is that under natural conditions, there is heat exchange in the surrounding
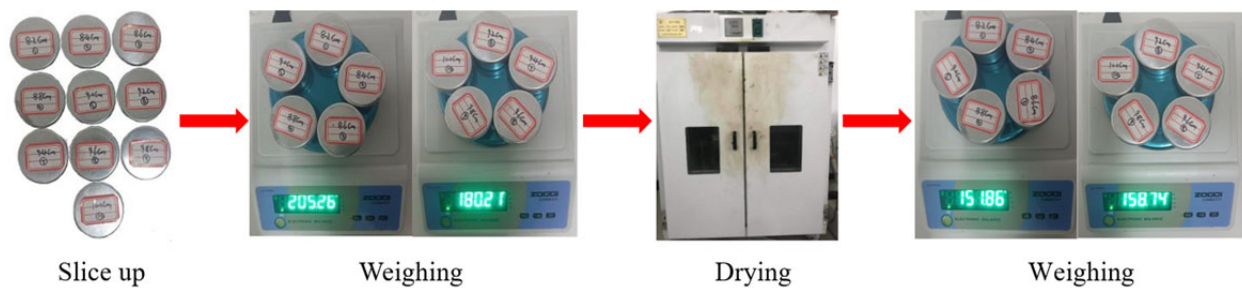

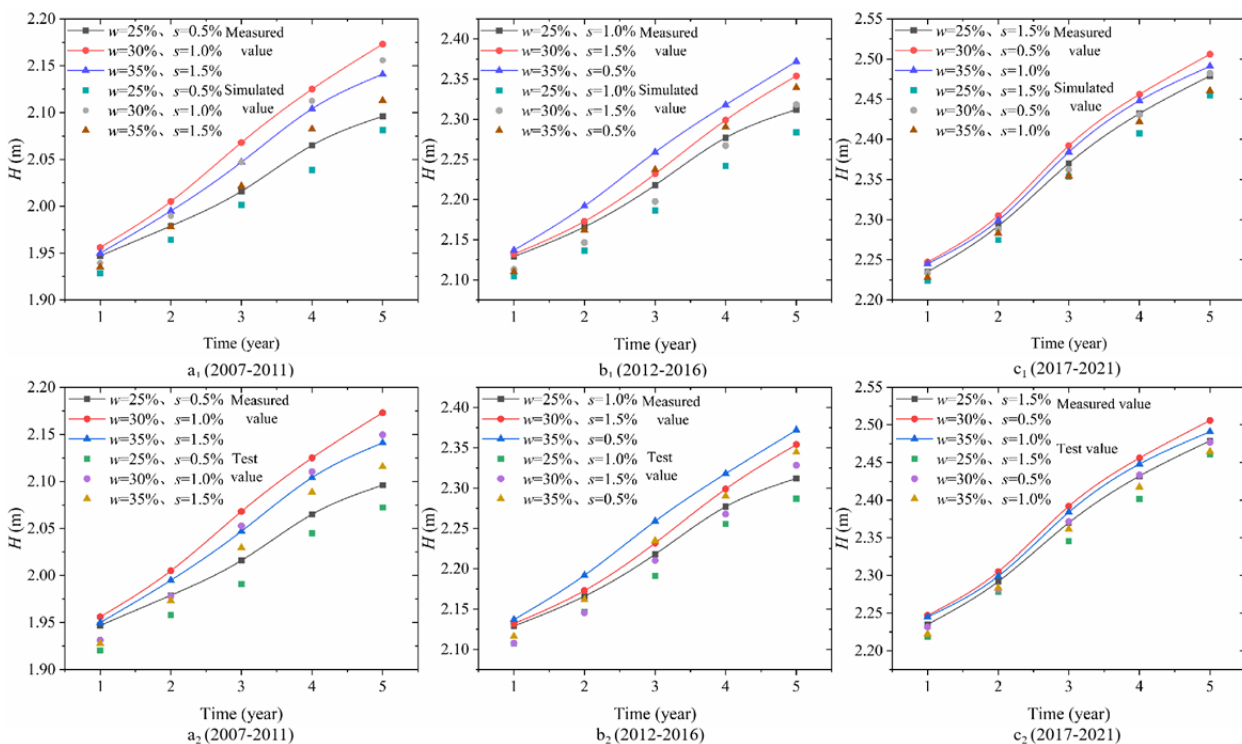**Fig. 7** Slice method to determine the maximum water content.

Fig. 8 Permafrost table determined by temperature. (a$_i$) H_0=1.92 m, (b$_i$) H_0=2.1 m, (c$_i$) H_0=2.2 m (H_0: Initial permafrost table).

soil, while the permafrost model is insulated, and the temperature can only be conducted from top to bottom. Under test conditions, there is heat loss.

Under the same temperature condition, the permafrost table becomes larger with the increase of soil water content and the decrease of soil salt content. Because the soil with high water content conducts heat well, which can carry a lot of heat to increase the depth of soil melting. However, an increase in salt content reduces the freezing temperature of the soil. As the salt content of the soil increases, the more salt ions in the aqueous soil solution, the more ions and water molecules participate in the hydration process, making the unfrozen water content lower, resulting in increased suction in the soil matrix, making the freezing process more difficult and the final freezing temperature lower.

In Figs. 8(a₁)~8(c₁), the average errors between the permafrost table determined by simulation and the field measured value in different years were 1.05%, 0.97% and 0.89%, respectively. In Figs. 8(a₂)~8(c₂), the average errors between the permafrost table determined by the test and the field measured value were 1.06%, 1.11% and 0.92%, respectively. All errors were within an acceptable range (Sun et al. 2014), which proved the correctness of determining the position of the permafrost table by temperature index. And the higher the temperature, the more accurate of permafrost table obtained by temperature index. The simulation results were better than the test results. The calculation of the errors, which can be expressed as Eq. (20).

$$\frac{|TP_a/TP_b - TP_o|}{TP_o} = E \qquad (20)$$

where TP_a is simulated value of permafrost table (m); TP_b is test value of permafrost table (m); TP_o is measured value of permafrost table (m); E is error (%).

From 2007 to 2011, the minimum difference and the maximum difference of the permafrost table obtained by simulation and test were 0.21 cm and 1.18 cm, respectively. Compared with the field measured values under the same conditions, the errors were 0.1% and 0.59%, respectively. From 2012 to 2016, the minimum difference and the maximum difference of the permafrost table obtained by simulation and test were 0.05 cm and 1.79 cm, respectively. Compared with the field measured values under the same conditions, the errors were 0.02% and 0.82%, respectively, and from 2017 to 2021, the minimum

difference and maximum difference of the value of the permafrost table obtained by simulation and test were 0.1cm and 1.56 cm, respectively. Compared with the field measured values under the same conditions, the errors were 0.04% and 0.2%, respectively, which were within the allowable range of errors. The results further proved the correctness of determining the position of the permafrost table by temperature.

5.2 Permafrost table determined by moisture

In Fig. 9, in the natural environment, when too much rain falls on the surface of the permafrost, the moisture seeps into the seasonal freeze-thaw layer and, due to the increase in moisture, resulting in a reduction in the rate of heat transfer from the soil, increasing the rate of permafrost melting and making the permafrost table larger. As there was no simulated rainfall in the simulated and experimental conditions, the permafrost table values obtained were smaller than the actual measured values in the field.

In Figs. 9(a₁)~9(c₁), the average errors between the permafrost table determined by simulation and the field measured value in different years were 1.38%, 1.29% and 1.17%, respectively. In Figs. 9(a₂)~9(c₂), the average errors between the permafrost table determined by the test and the field measured value were 1.36%, 1.33% and 1.23%, respectively. All errors were within the allowable range of engineering error, which proved the correctness of determining the position of the permafrost table by moisture index. With the increase in temperature, the error of the permafrost table obtained by moisture decreased. From Fig. 8 and Fig. 9, the permafrost table determined by temperature index was closer to the measured value than that determined by moisture. The reason was that the change of the permafrost table was due to the change of the unfrozen water content caused by the change of soil temperature, and the permafrost was melted by the heat carried by moisture. The temperature was the most important and direct factor for the change of the permafrost table, so the soil was more sensitive to the temperature change, and the permafrost table obtained by the temperature index was more accurate.

From 2007 to 2011, the minimum difference and the maximum difference of the permafrost table obtained by simulation and test were 0.04cm and 0.95cm, respectively. Compared with the field measured values under the same conditions, the
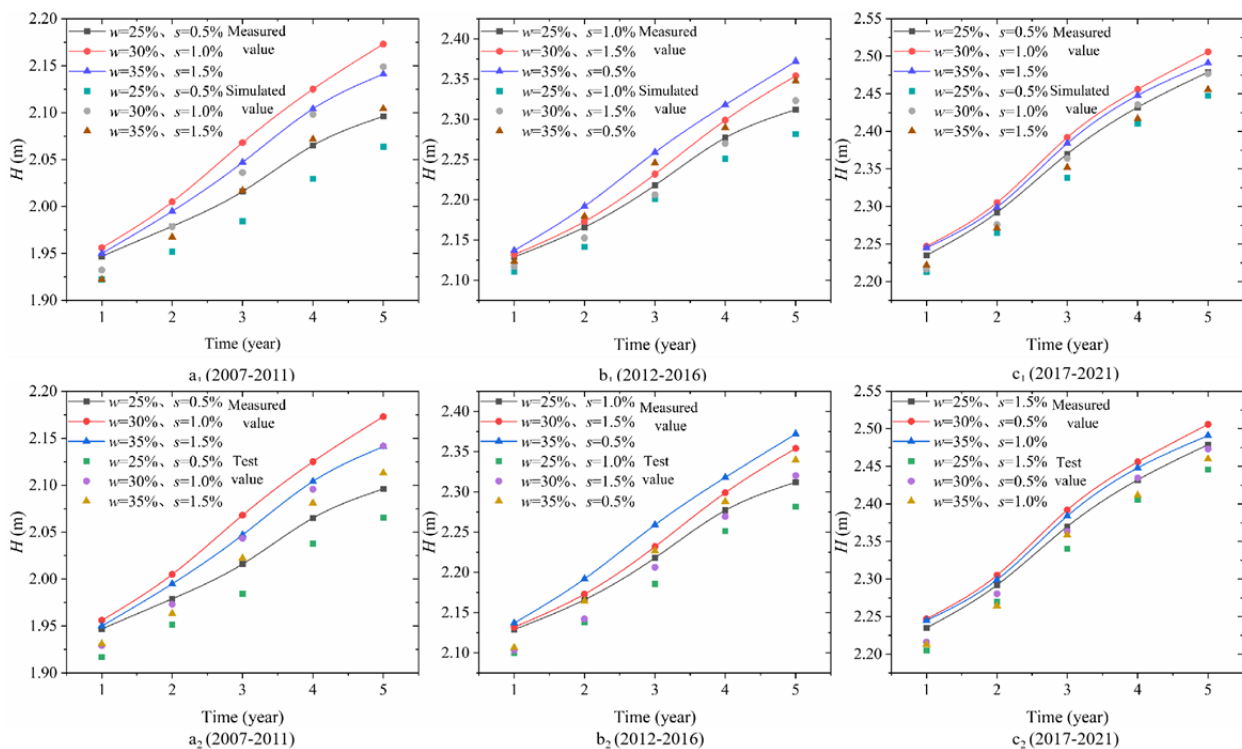
Fig. 9 Permafrost table determined by moisture. (a_i) H_0=1.92 m, (b_i) H_0=2.1 m, (c_i) H_0=2.2 m (H_0: Initial permafrost table).

errors are 0.02% and 0.45%, respectively. From 2012 to 2016, the minimum difference and the maximum difference of the permafrost table obtained by simulation and test were 0.09cm and 1.04cm, respectively. Compared with the field measured values under the same conditions, the errors were 0.04% and 0.46%, respectively, and from 2017 to 2021, the minimum difference and maximum difference of the value of the permafrost table obtained by simulation and test were 0.07cm and 0.9cm, respectively. Compared with the field measured values under the same conditions, the errors were 0.03% and 0.4%, respectively, which were within the allowable range of errors. The results further proved the correctness of determining the position of the permafrost table by moisture.

5.3 Permafrost table determined by salt content

In Fig. 10, the values of the permafrost table obtained by simulation and test were greater than the field measured values. A large number of unfrozen water and salt move to the freezing front during the freezing process under natural conditions. With the increase in temperature, the evaporation of water from the upper surface of the seasonal freeze-thaw layer increases the concentration of the salt solution in the soil, and salt above the saturation level will crystallise and precipitate, these salt crystals will fill the voids in the permafrost, resulting in a decrease in the porosity of the permafrost, thus impeding the flow of permeable water in the permafrost. However, the salt content was constant under simulation and test, so the values of the permafrost table obtained through simulation and test were greater than the measured values.

In Figs. 10(a_1)~10(c_1), the average errors between the permafrost table determined by simulation and the field measured value in different years were 1.72%, 1.46% and 1.36%, respectively. In Figs. 10(a_2)~10(c_2), the average errors between the permafrost table determined by the test and the field measured value in different years were 1.99%, 2.06% and 2.08%, respectively. All errors were within the allowable range of engineering error, which proved the correctness of determining the position of the permafrost table by salt content. With the increase of temperature, the error of the permafrost table determined by salt content decreased. From Figs. 8-10, the error between the value of the permafrost table determined by salt content and the measured value was the largest. The reason was that the change of salt
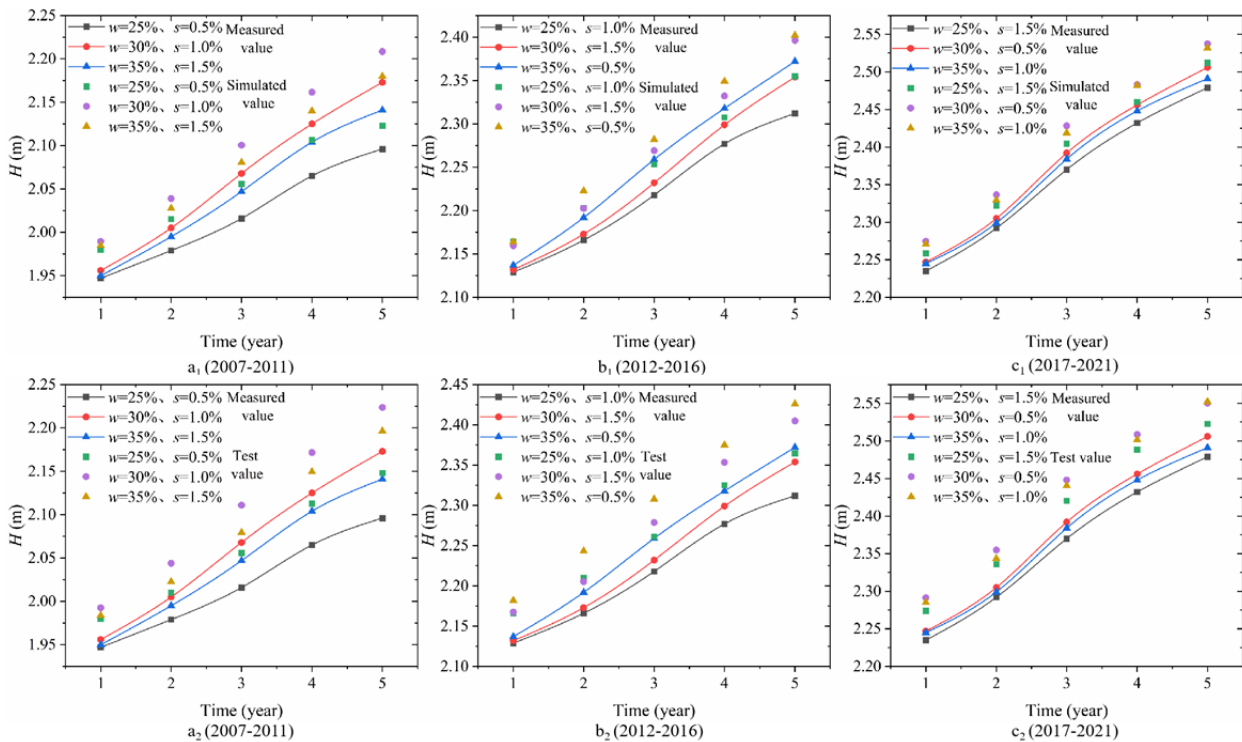
Fig. 10 Permafrost table determined by salt content. (a_i) H_0=1.92 m, (b_i) H_0=2.1 m, (c_i) H_0=2.2 m (H_0: Initial permafrost table).

content in soil changes with the migration of moisture. The migration of water was caused by the change of temperature. The influence of salt on the permafrost table was the weakest in the freezing and thawing process of soil. Therefore, the error of the value of the permafrost table determined by the salt index was the largest.

From 2007 to 2011, the minimum difference and the maximum difference of the permafrost table obtained by simulation and test were 0.06cm and 2.51cm, respectively. Compared with the field measured values under the same conditions, the errors were 0.03% and 1.2%, respectively. From 2012 to 2016, the minimum difference and the maximum difference of the permafrost table obtained by simulation and test were 0.19cm and 2.58cm, respectively. Compared with the field measured values under the same conditions, the errors were 0.09% and 1.14%, respectively, and from 2017 to 2021, the minimum difference and maximum difference of the value of the permafrost table obtained by simulation and test were 1.04cm and 2.85cm, respectively. Compared with the field measured values under the same conditions, the errors were 0.43% and 1.17%, respectively, which were within the allowable range of errors. The results further proved

the correctness of determining the position of the permafrost table by salt.

6 Determination of Indexes for Judging the Permafrost Table

6.1 Error analysis of simulations and tests

The changes of temperature, moisture and salt content in the soil were used as the indexes to determine the position of the permafrost table. The values of the permafrost table determined by the three indexes were compared with the field measured values, and the errors for different indexes were obtained, as shown in Fig. 11.

In Fig. 11, all errors between the values of the permafrost table determined by temperature, moisture and salt content and the field measured values were less than 3%, which was within the allowable range of errors. And this proved the correctness of the method for determining the position of the permafrost table. The errors of the permafrost table obtained by simulation were less than the test. This showed that it was more accurate to determine the permafrost table through simulation.
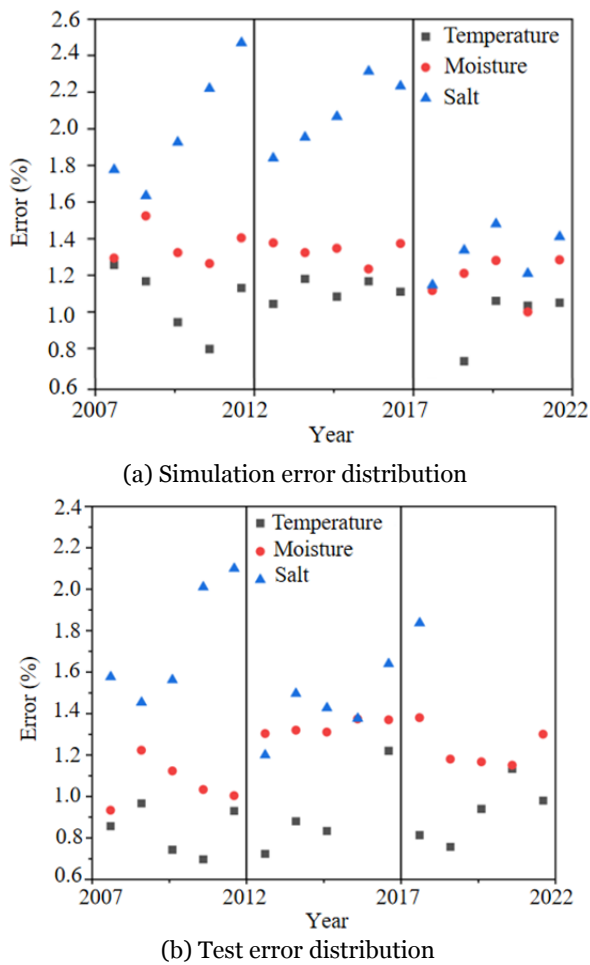
(a) Simulation error distribution

(b) Test error distribution

Fig. 11 Error distribution of permafrost table determined by different indexes.

Under the conditions of simulation and test, the average error of permafrost table value determined by temperature index was between 0% to 1.26%; the average error determined by moisture index was between 0% to 1.52%; and the average error determined by the salt index was between 0% to 2.47%, which proved the superiority of temperature in determining the position of permafrost table, followed by moisture and salt.

6.2 Error analysis of single and multiple indexes

In Section 6.1, the error in determining the permafrost table using the temperature indexes was minimized under numerical simulation. The error in the permafrost table obtained from a single temperature index was compared with the error in the permafrost table obtained by averaging the three indexes, as shown in Fig. 12.

In Fig. 12, errors in determining the permafrost table for single temperature were all greater than those determined by average of the three indexes. In order to reduce the influence of external factors on the final results and help to obtain more accurate permafrost table, we used the average value obtained from three indexes as the final permafrost table.
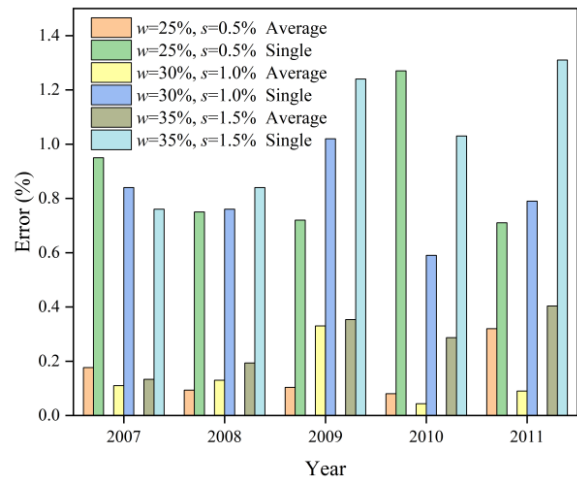

Fig. 12 Comparison of errors in results for single and average indexes.

6.3 Validation of the suitability of the simulation

In order to validate the applicability of determining permafrost table by temperature, moisture and salt content under different conditions, the change of permafrost table under different conditions was simulated. And the errors of the permafrost table determined by different indexes under different conditions were obtained and compared with the field measured values. The heating rates were set as 0.16°C/a, 0.1°C/a, 0.06°C/a and 0.025°C/a, respectively. The water content was set as 25%, 30%, 35% and 40%, respectively. The salt content was set as 0.5%, 1%, 2% and 3%, respectively. Error variation curves were shown in Figs. 13-15.

In Fig. 13, with the increase of temperature, the error between the permafrost table determined by three different indexes and the field measured values becomes smaller. Because permafrost is highly susceptible to temperature, as the temperature increases, the temperature gradient of soil changes faster, so the permafrost table is more accurately determined by temperature. The temperature gradient affects the moisture migration, and the time of soil melting decreases with the increase of
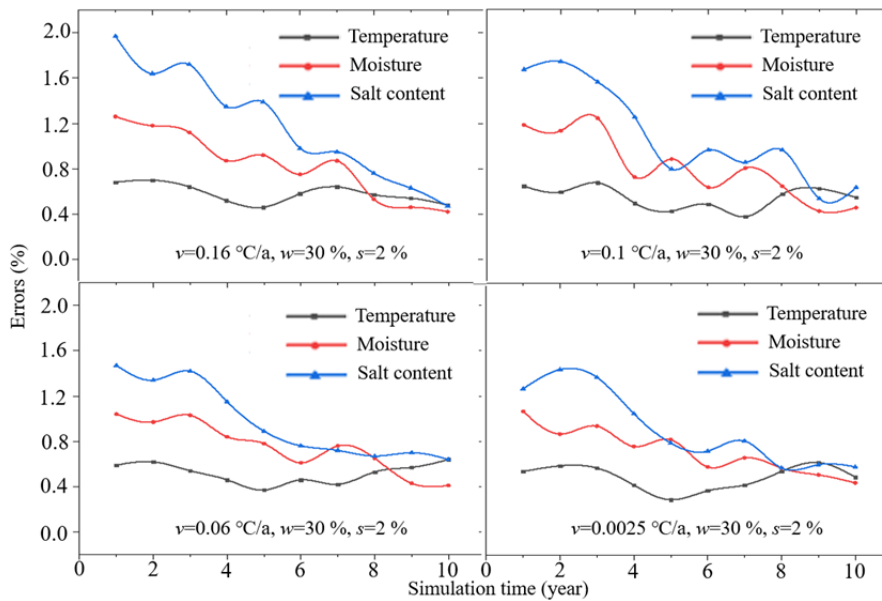
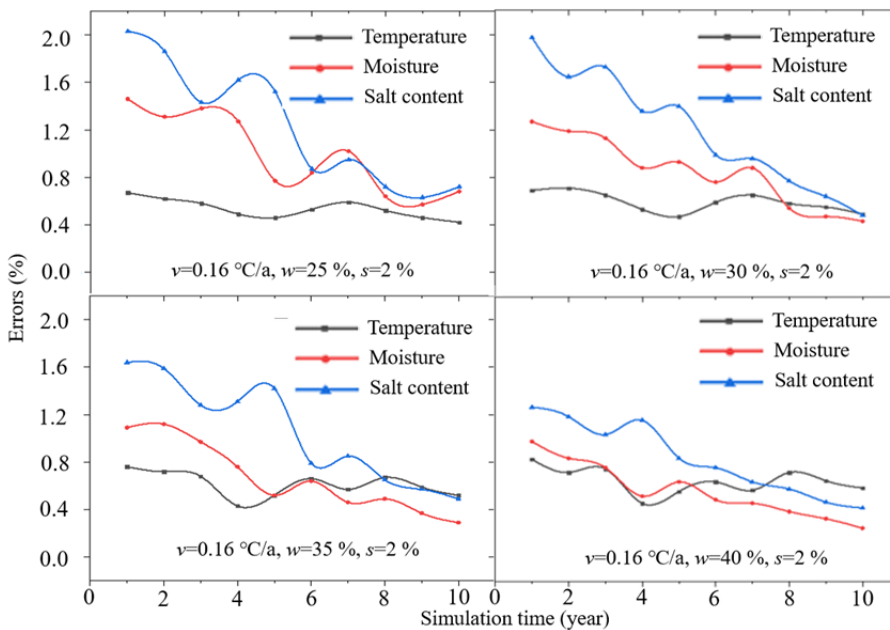**Fig. 13** Error analysis of permafrost table under different temperatures.

Fig. 14 Error analysis of permafrost table under different moisture conditions.

error of the permafrost table determined by temperature gradually increases, while the error of the permafrost table determined by moisture and salt content gradually decreases. Finally, the permafrost table determined by moisture is the closest to the measured value, followed by temperature and finally salt content. The reason is that the increased moisture accumulates more near the permafrost table under the action of self-weight. Then, the moisture distribution gradient in the soil becomes larger, which can more accurately determine the maximum position of soil water content. However, salt migrates with moisture in the soil. The increase of water content makes it more convenient for salt to migrate with moisture, and more salt accumulates at the top of permafrost. Thus, moisture is more accurate to determine the permafrost table. Meanwhile, the increase of water content slows down the conduction of temperature in the soil, and the position difference of 0°C isotherm deviates, which weakens the accuracy of temperature as an index for determining permafrost table.

In Fig. 15, with the increase of salt content, the errors of permafrost table determined by moisture and salt content become smaller, and the errors of permafrost table determined by temperature become larger. The reason is that with the increase of initial salt content, the freezing temperature of soil will gradually decrease, The temperature at the location of the permafrost table is below 0°C at this time due to the effect of salt, so choosing the depth from the

temperature. Under gravity, the moisture accumulates more near the permafrost table. The salt migrates downward with moisture, and its variation law is consistent with moisture, so the errors determined by moisture and salt content also decrease.

In Fig. 14, when the moisture is 25%-35%, the maximum error of the permafrost table determined by temperature is the minimum, thus, temperature is the most reliable index to determine the position of the permafrost table. With the increase of moisture, the

location of 0°C to the surface as the value of the permafrost table will give a small result, and the soil will start to melt under the condition of negative temperature. When the salt content of soil increases, the melting temperature of ice will decrease. There is no doubt that the error will gradually increase. When 0°C is still used to determine the position of the permafrost table, the melting time of soil is much earlier. More moisture is concentrated at the maximum melting depth. At this time, it is more accurate to determine the position of the permafrost table by moisture. When the salt content is more, the difference of salt distribution in the soil is greater, which can more accurately determine the maximum salt accumulation.

Fig. 15 Error analysis of permafrost table under different salt content conditions.

6.4 Engineering applicability validation of simulation

In order to further verify the engineering applicability of the method to determine the permafrost table, the Mado, Qilian Mountains and Thermokarst Lake of the Qinghai-Tibet Plateau were selected and numerical simulations were carried out based on the parameters of permafrost provided in the literature (Cao et al. 2014; Sun 2022; Ke et al. 2022). The values of the permafrost table obtained were compared with the field measured values, and the error results obtained, as shown in Fig. 16.

In Fig. 16, the errors between the permafrost table values obtained in different areas and the field measured values were less than 3%, which showed that the method was suitable for determining the location of the permafrost table in different regions. Compared with the traditional drilling method, our method has a shorter construction period and does not damage the local ecosystem; compared with the radar detection method, it does not need to be determined by field tests; and compared with the empirical formula method, our method has less error and high reliability.
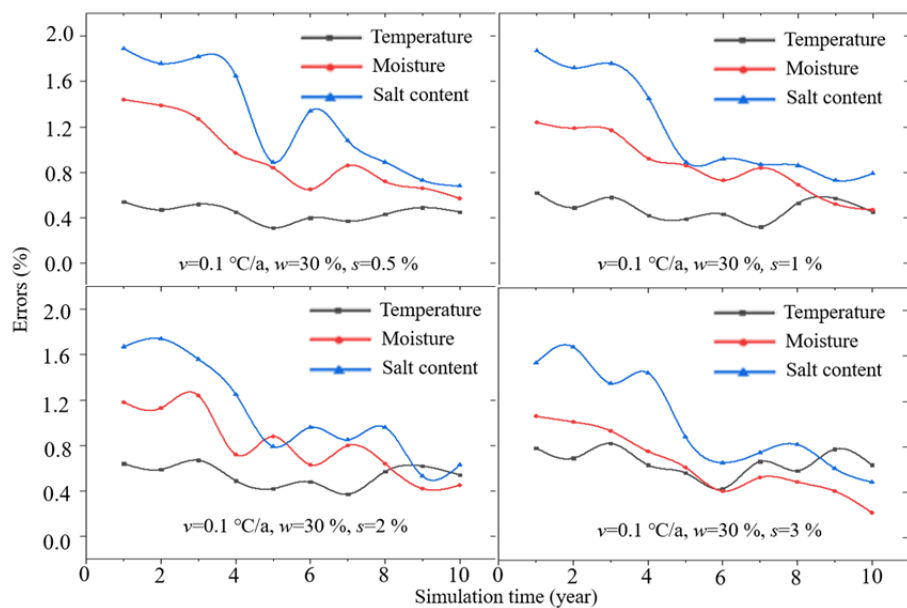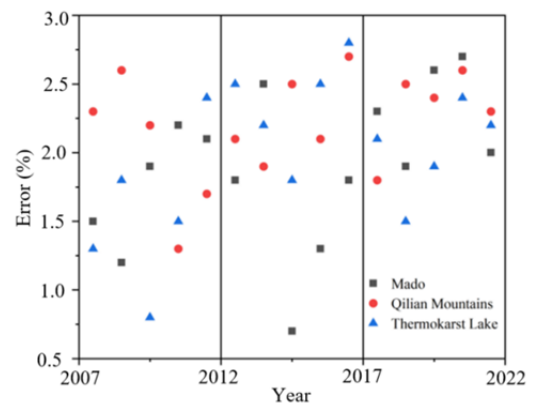

Fig. 16 Error distribution of permafrost table determined by different regions.

7 Conclusions

Based on the water, heat and salt transfer law of permafrost under natural conditions, a method for determining the permafrost table based on changes of temperature, moisture and salt content was proposed. The permafrost model was established according to the similarity theory, and the permafrost table under different simulation conditions was obtained through a finite element solution. An accelerated permafrost table test with enclosure space, constant pressure and no moisture supplement was designed, and the permafrost table under different test conditions was obtained. The permafrost table obtained under simulated and experimental conditions was verified

by field measured value, which proved the correctness of the method for determining the permafrost table. The conclusions are as follows:

(1) With the increase of freezing and thawing time, the permafrost table gradually increases and eventually stabilizes, and the increase rate gradually decreases. The permafrost table determined by average of three indexes the was closest to the field measured value, followed by temperature, moisture and salt content. With the increase of temperature, the error between the permafrost table determined by three indexes and the field measured value gradually decreases.

(2) The permafrost table determined by temperature and moisture was less than the field measured value, and the permafrost table determined by salt content was greater than the field measured value.

(3) Through simulation, the errors of the permafrost table determined by temperature, moisture and salt content were 0.97%, 1.28% and 1.5% respectively, while the errors of the permafrost table determined by the test were 1.03%, 1.6%, and 2.04%, respectively. The errors of the permafrost table determined by simulation were smaller than by test, and all errors were less than 3.0% and within the allowable error range, which proved the feasibility and accuracy of the permafrost table determination method.

(4) The errors of the permafrost table were determined by different indexes under the condition of single factor change. With the increase of temperature, the errors of the permafrost table determined by different indexes gradually decrease, and the temperature index was superior to moisture and salt content. With the increase of moisture or salt content, the errors of the permafrost table determined

by temperature increase. When the moisture was more than 35% and the salt content was more than 2%, the permafrost table determined by moisture was more accurate than temperature. The error of the permafrost table determined by salt content was the largest under any conditions.

Acknowledgments

Author Contribution

All authors contributed to the study conception and design. Material preparation, data collection and analysis were performed by YANG Zhong and LU Chang-long. The first draft of the manuscript was written by WANG Fang, LIU Kai and YANG Zhong, and all authors commented on previous version of the manuscript. All authors read and approved the final manuscript.

Ethics Declaration

Availability of Data/Materials: Data will be made available from the corresponding author on request.

Conflict of Interest: The authors declare no conflict of interest.

References

Bing H, He P, Zhang Y (2015) Cyclic freeze-thaw as a mechanism for water and salt migration in soil. Environ Earth Sci 74(1): 675-681.
https://doi.org/10.1007/s12665-015-4072-9

Cao YB, Sheng Y, Wu J, et al. (2014) Influence of upper boundary conditions on simulated ground temperature field in permafrost regions. J Glaciol Geocryol 36(4): 802-810. (In Chinese)
http://www.bcdt.ac.cn/CN/10.7522/j.issn.1000-0240.2014.0096

Dobinski W (2020) Permafrost active layer. Earth-Sci Rev 208.
https://doi.org/10.1016/j.earscirev.2020.103301

Daout S, Doin M, Peltzer G, et al. (2017) Large-scale InSAR monitoring of permafrost freeze-thaw cycles on the Tibetan Plateau. Geophys Res Lett 44(2): 901-909.
https://doi.org/10.1002/2016GL070781

Dong WC, Cui S, Fu Q, et al. (2018) Modelling soil solute release and transport in run-off on a loessial slope with and without surface stones. Hydrol Process 32(10): 1391-1400.
https://doi.org/10.1002/hyp.11497

Genuchten MTV (1980) A closed-from equation for predicting the hydraulic conductivity of unsaturated soils. Soil Sci Soc Am J 44(5): 892-898.
https://doi.org/10.2136/sssaj1980.03615995004400050002x

Harlan RL (1973) Analysis of coupled heat-fluid transport in partially frozen soil. Water Resour Res 9(5): 1314-1323.
https://doi.org/10.1029/WR009i005p01314

Jia YY, Kim JW, Shum C, et al. (2017) Characterization of active

layer thickening rate over the notthem Qinghai-Tibetan Plateau permafrost region using ALDS interferometric synthetic aperture radar data. Remote Sen 9(1).
https://doi.org/10.1002/2016GL070781

Jin DW, Niu FJ, Cheng ZX (2004) Simulation analysis for model experiment of frozen soil slope. J Earth Sci Environ (1): 29-32. (In Chinese)
https://www.docin.com/p-851244384.html

Jia BX, Yang CF, Wang H, et al. (2020) Experimental study on frost heaving characteristics of silty soil under closed and non-hydrating conditions. J Liaoning Tech Univ Nat Sci Ed 39(3): 219-225.
https://doi.org/10.11956/j.issn.1008-0562.2020.03.005

Ji Y, Zhou GQ, Zhao XD, et al. (2017) On the frost heaving-induced pressure response and its dropping power-law behaviors of freezing soils under various restraints. Cold Reg Sci Technol 142: 25-33.
https://doi.org/10.1016/j.coldregions.2017.07.005

Kong XB, Guy D, Fabrice C (2018) Thermal modeling of heat balance through embankments in permafrost regions. Cold Reg Sci Technol 158: 117-127.
https://doi.org/10.1016/j.coldregions.2018.11.013

Ke XM, Ou AF, Wang W et al. (2014) Interaction of thermokarst lake and permafrost in Qinghai-Tibet Plateau. Adv Water Resour 33(4): 542-552. (In Chinese)
https://doi.org/10.14042/j.cnki.32.1309.2022.04.003

Liu WB, Yu WB, Hu D, et al. (2019) Crack damage investigation of paved highway embankment in the Tibetan Plateau permafrost environments. Cold Reg Sci Technol 163: 78-86.
https://doi.org/10.1016/j.coldregions.2019.05.003

Lu N, Likos WJ (2004) Unsaturated soil mechanic, USA. John Wiley & Sons.
https://www.wiley.com/en-us/Unsaturated+Soil+Mechanics-p-9780471447313

Ming F, Li DQ (2016) A model of migration potential for moisture migration during soil freezing. Cold Reg Sci Technol 124: 87-94.
https://doi.org/10.1016/j.coldregions.2015.12.015

Obu J (2021) How much of the earth's surface is underlain by permafrost? J Geophys Res: Earth Surf 126(5).
https://doi.org/10.1029/2021JF006123

Peng H, Ma W, Mu YH, et al. (2015) Impact of permafrost degradation on embankment deformation of Qinghai-Tibet highway in permafrost regions. J Cent South Univ (Engl Ed) 22(3):1079-1086.
https://doi.org/10.1007/s11771-015-2619-2

Qi S, Li G, Chen D, et al. (2023) Research on the characteristics of thermosyphon embankment damage and permafrost distribution based on ground-penetrating radar: A case study of the Qinghai-Tibet highway. Remote Sens 15(10).
https://doi.org/10.3390/rs15102651

Ryan C, Élise D, Masaki H, et al. (2018) The influence of shallow taliks on permafrost thaw and active layer dynamics in subarctic Canada. J Geophys Res: Earth Surf 123(2): 281-297.
https://doi.org/10.1002/2017JF004469

Romanovsky VE, Drozdov DS, Oberman NG, et al. (2010) Thermal state of permafrost in Russia. Permafrost Periclac 21(2): 136-155.
https://doi.org/10.1002/ppp.683

Rasmussen LH, Zhang WX, Hollesen J, et al. (2018) Modelling present and future permafrost thermal regimes in Northeast Greenland. Cold Reg Sci Technol 146: 199-213.
https://doi.org/10.1016/j.coldregions.2017.10.011

Ren CJ, Bai D, He F, et al. (2017) Study of hydrodynamic dispersion coefficient in unsaturated soil. J Xi'an Technol Univ 33: 419-424. (In Chinese)
https://doi.org/10.19322/j.cnki.issn.1006-4710.2017.04.008

Shiklomanov NI, Streletskiy DA, Little JD, et al. (2013) Isotropic thaw subsidence in undisturbed permafrost landscapes.

Geophys Res Lett 40(24): 6356-6361.
https://doi.org/10.1002/2013GL058295

Shafique U, Anwar J, Munawar MA (2016) Chemisty of ice: Migration of ions and gasws by directional freezing of water. Arab J Chem 9: 47-53.
https://doi.org/10.1016/j.arabjc.2011.02.019

Sun QS, Chang JF (2014) Thaw settlement prediction of permafrost subgrade based on support vector machine. Highway Engineer 39(05):136-140+148. (In Chinese)
https://kns.cnki.net/kcms2/article/abstract?v=3uoqIhG8C44YLTlOAiTRKgchrJo8w1e7M8Tu7YZds8-O_OZTp_C13OAWEkeTN3lSdxFj9ED7cucXYGTf5iRS1Vi8Z2gQjz4q&uniplatform=NZKPT

Sun W (2022) Permafrost simulation in the Qilian Mountains over the upper reaches of Heihe River Basin. PHD thesis, Lanzhou University, Lanzhou, Gansu Province. (In Chinese)
https://doi.org/10.27204/d.cnki.glzhu.2022.003656

Vereecken H, Weynants M, Javaux M, et al. (2010) Using pedotransfer functions to estimate the van genuchten-mualem soil hydraulic properties: a review. Vadose Zone J 9(4): 795-820.
https://doi.org/10.2136/vzj2010.0045

Wan HL, Bian JM, Zhang H, et al. (2021) Assessment of future climate change impacts on water-heat-salt migration in unsaturated frozen soil using coupmodel. Front Environ Sci Eng 15(1).
https://doi.org/10.1007/s11783-020-1302-5

Xu C, Liao XY, Ye GB, et al. (2005) Research on effective cement-soil mixing pile length by load tests. Hydrogeol Eng Geol (03):103-104+107. (In Chinese)
https://doi.org/10.16030/j.cnki.issn.1000-3665.202007042

Xu J, Lan W, Li YF, et al. (2020) Heat, water and solute transfer in saline loess under uniaxial freezing condition. Comput Geotech 118:103319.
https://doi.org/10.1016/j.compgeo.2019.103319

Xu XZ, Wang JC, Zhang LX, et al. (2001) Permafrost Physics, Beijing, China. Science Press. pp 39-97. (In Chinese)
https://book.sciencereading.cn/shop/book/Booksimple/show.do?id=BB94387E3BD4A435BB86FEEA35B69F5F6000

Yang YZ, Wu QB, Jang GL, et al. (2018) Ground ice at depths in the Tianshuihai Lake basin on the western Qinghai -Tibet Plateau: An indication of permafrost evolution Sci Total Environ 729:138966.
https://doi.org/10.1016/j.scitotenv.2020.138966

Zhao DS, Wu SH (2019) Projected changes in permafrost active layer thickness over the Qinghai-Tibet Plateau under climate change. Water Resour Res 55(9): 7860-7875.
https://doi.org/10.1029/2019WR024969

Zhang J, Lai YM, Li JF, et al. (2020) Study on the influence of hydro-thermal-salt-mechanical interaction in saturated frozen sulfate saline soil based on crystallization kinetics. Int J Heat Mass Transfer 146:118868.
https://doi.org/10.1016/j.ijheatmasstransfer.2019.118868

Zhang Z, Li X, Zhang Y (2022) Variation of permafrost upper limit in permafrost subgrade covered by snow on steep slope of Alpine Mountains. Shock Vib 1-11.
https://doi.org/10.1155/2022/8706397

Zhu ZY, Tang CX, Ma Y, et al. (2022) Train-induced vibration and subsidence prediction of the permafrost subgrade along the Qinghai-Tibet railway. Soil Dyn Earthq Eng 162.
https://doi.org/10.1016/j.soildyn.2022.107433

Zhou JQ (1999) Heat transfer, Beijing, China. Metallurgy Industry Press. pp 150-152. (In Chinese)

Jia BX, Yang CF, Wang H, et al. (2020) Experimental study on frost heaving characteristics of silty soil under closed and non-hydrating conditions. J Liaoning Tech Univ Nat Sci Ed 39(3): 219-225.
https://doi.org/10.11956/j.issn.1008-0562.2020.03.005